JOURNAL OF MATERIALS SCIENCE 25 (1990) 1551–1556

SAXS experiments on voids in gel-spun polyethylene fibres

W. HOOGSTEEN, G. TEN BRINKE, A. J. PENNINGS
Department of Polymer Chemistry, University of Groningen, Nijenborgh 16, 9747 AG Groningen, The Netherlands

The morphology and properties of extracted gel-spun polyethylene fibres depend on the spinning conditions. The main structures in the extracted fibre are shish-kebabs and lamellae. Equatorial small-angle X-ray scattering (SAXS) experiments show that the former structure is very porous due to the presence of lamellar overgrowth preventing a close package of the backbone fibrils, whereas the latter structure is relatively dense. After hot-drawing, due to melting/recrystallization, both structures are transformed on a 100 nm scale into a dense structure consisting of shish-kebabs or fibrils containing a void volume fraction of about 1%, as revealed by the scattering power of equatorial SAXS experiments. Moreover, a slight decrease of the equatorial intensity especially at the smallest angles after treating the hot-drawn fibres with paraffin oil, points to a small contribution of multiple scattering to the equatorial scattering. This implies the presence of a superstructure of not too closely packed macrofibrils. SAXS measurements of strained ultra-high-strength polyethylene fibres show that no or very little void formation is involved in the fracture mechanism. Most probably this is due to the (partly) fibrillar structure.

1. Introduction

The presence of flaws in fibres strongly affect their properties, because stress concentrations at these flaws result in premature breakage. There are several types of flaws such as crystal defects, folds, trapped entanglements, kinks and voids [1, 2]. The presence of voids in fibres can be demonstrated by electron microscopy, density measurements or small-angle X-ray scattering (SAXS). The latter technique was used for cellulose fibres [3–6], carbon fibres [7–11] and poly(*p*-phenylene terephthalamide) fibres [12, 13]. The morphology of these fibres consists of not too closely packed fibrillar structures elongated in the fibre axis direction, and the voids are therefore also elongated in the same direction. Another type of void is found in crystalline polymer fibres/films subjected to mechanical stresses. Examples are oriented polyethylene [14], unoriented polyoxymethylene [15, 16] and hard elastic fibres [17, 18]. These voids are more or less rotational ellipsoids with the smallest axis parallel to the draw direction. Here, local high stress concentrations at flaws are responsible for the void formation. A similar behaviour is found for amorphous polymers where a void structure with voids spanned by fibrils in the direction of drawing due to crazing is obtained [19–21].

In this paper the results of a small-angle X-ray scattering study of voids in gel-spun polyethylene fibres are presented. The gel-spinning method used in our laboratory to produce ultra-high-strength polyethylene fibres consists of extrusion of a 1 to 5 wt % polyethylene solution in paraffin oil through a conical die followed by quenching in air. Afterwards, the paraffin oil is removed by extraction with *n*-hexane and the fibre is subsequently dried. This yields very porous fibres. Finally, the extracted fibre is hot-drawn which can be accompanied by a large improvement of the fibre properties. During this step, the porosity of the fibre diminishes. In this study the porosity of the extracted, as well as the hot-drawn, fibres will be discussed. Moreover, the role of void formation with respect to the fracture mechanism will be considered.

2. Experimental details

Two samples of linear polyethylene Hifax 1900 were used, one with a broad molecular weight distribution ($\bar{M}_w = 4 \times 10^6$ kg kmol^{-1}, $\bar{M}_w/\bar{M}_n \approx 20$; referred to as Hifax A) and one with a narrow molecular weight distribution ($\bar{M}_w = 5.5 \times 10^6$ kg kmol^{-1}, $\bar{M}_w/\bar{M}_n \approx 3$; referred to as Hifax B). 1 to 5 wt % polyethylene solutions in paraffin oil were prepared (containing 0.5 wt % 2,6-di-*t*-butyl, *p*-methylcresol anti-oxidant) at 150° C. Upon cooling this solution forms a gel which was fed to the spinning apparatus. The gel was extruded into a filament at temperatures varying from 170 to 250° C with an extrusion rate of 1 or 100 m min^{-1} using a conical die with an exit of 1 mm [22]. The paraffin oil was extracted from these filaments with *n*-hexane. Afterwards hot-drawing to different draw ratios was carried out at a temperature in the range 144 to 148° C in a nitrogen atmosphere.

For the small-angle X-ray scattering experiments CuKα radiation ($\lambda = 0.154$ nm) was used, produced by a Philips X-ray generator connected to a closed cooling circuit and operated at 45 kV and 45 mA.

0022–2461/90 $03.00 + .12

SAXS experiments were carried out with the aid of a Kratky camera equipped with a proportional counter and an electronic stepscanner. Monochromatization was achieved by using a nickel filter and pulse height discrimination. The entrance slit was 80 μm. In the case of equatorial measurements, one fibre was aligned accurately with the fibre axis parallel to the slit, whereas for meridional measurements fibres were placed next to each other over the length of the X-ray beam perpendicular to the plane of the beam by winding a fibre on a rectangular frame. In the last case many cross-sections are irradiated. It should be noticed that in this way two layers of fibres are obtained, slightly displaced by the frame thickness and that the fibre turns are inclined a little with respect to the vertical as a result of the pitch. In some cases SAXS experiments were also carried out with a Statton camera (pinhole collimation; sample to film distance 31 cm and using a bundle of fibres).

3. Results and discussion

3.1. Voids in extracted gel-spun polyethylene fibres

The presence of voids in the extracted gel-spun polyethylene fibres is well known. Its high scattering contribution complicates the study of the morphology of the extracted fibres [23, 24]. The formation of porous structures can be ascribed to two facts. In the first place, the use of the volatile *n*-hexane for the extraction process results in a very fast, but incomplete, lateral shrinkage during the evaporation of hexane [23]. This process is, in particular, of interest for fibres containing a lamellar structure. For fibres with a shish-kebab structure the lamellar overgrowth prevents a close packing of the fibrils [23].

The porous fibres may be considered as a three-phase system consisting of amorphous polyethylene, crystalline polyethylene and voids with electron densities, ϱ, of 0.489, 0.571 and 0 mol electron cm^{-3}, respectively. The scattering power $\overline{\eta^2}$ is given by

$$\overline{\eta^2} = \omega_c\omega_a(\varrho_c - \varrho_a)^2 + \omega_c\omega_v(\varrho_c - \varrho_v)^2 + \omega_a\omega_v(\varrho_a - \varrho_v)^2 \quad (1)$$

where ω_c, ω_a and ω_v are the volume fractions of crystalline polyethylene, amorphous polyethylene and voids. The square of the electron density difference of crystalline and amorphous polyethylene $(\varrho_c - \varrho_a)^2$ is very small (6.7×10^{-3} mol^2 electron^2 cm^{-6}) compared to the values for crystalline polyethylene/void and amorphous polyethylene/void (3.26×10^{-1} and 2.39×10^{-1} mol^2 electron^2 cm^{-6}, respectively). Therefore, the scattering contribution due to the crystalline/amorphous electron density difference can be relatively small. For example, for a crystallinity of the polyethylene of 60%, this contribution to the total scattering is 35.4% and 4.5% for void volume fractions of 1% and 10% respectively. The crystallinity of the extracted fibres is of the order of 60% to 70% as shown previously in our differential scanning calorimetry (DSC) study of gel-spun polyethylene fibres [25]. For a fibre with known crystallinity the volume fraction of voids can be calculated from the scattering power $\overline{\eta^2}$. It requires a determination of the absolute intensity which for some fibres is a little problematic due to very small lateral dimensions.

This problem can be avoided by filling the pores with paraffin oil with an electron density ϱ_p of 0.483 mol electron cm^{-3} (calculated from a density of 0.845 g cm^{-3}). Filling the pores eliminates the void scattering contribution to a large extent. If swelling is negligible and all the voids are filled with paraffin oil, the void volume fraction can be calculated from the ratio of the relative scattering power $\overline{\eta_v^2}/\overline{\eta_p^2}$ assuming the crystallinity is known ($\overline{\eta_v^2}$ and $\overline{\eta_p^2}$ are the "observed" scattering powers for the fibre before and after filling with paraffin oil). For example, the calculated ratios for a fibre with 60% crystallinity containing a volume fraction voids of 1%, 10% and 50% are 2.7, 15.9 and 46.7, respectively. The disadvantage of this method is that it is time consuming because it needs the determination of the scattering curve before and after filling the pores.

The slit-smeared equatorial scattering curves were scaled to an absolute intensity scale using a Lupolen polyethylene sample (in this paper only slit-smeared intensities are dealt with because desmearing is only possible for isotropic samples). The following procedure was used for fibres with a lateral dimension smaller than the width of the primary beam, which may occur for fibres stretched in the spinline (and, of course, also for the hot-drawn fibres considered in the next section). The primary beam profile in the direction perpendicular to the slit at the sample position is a triangular distribution in the case of complete illumination of the entrance slit as can be calculated from the dimensions of the Kratky collimation. This was checked by measuring the primary beam profile at the detector position using a 20 μm counter slit. The measured and calculated beam profile at the detector position agreed well. From the calculated triangular beam profile at the sample position, absolute intensities were estimated. First, the diameter was measured using a microscope and micrometer. For the equatorial scattering experiments the fibres were aligned accurately with the fibre axis parallel to the slit in such a way that the highest intensity was obtained. The limited width of the fibre was taken into account by using only the relevant part of the primary beam at the sample position. In this way a reasonable approximation of the absolute intensities could be obtained for fibres with a lateral dimension exceeding 35 μm. For fibres with an even smaller width, additional complications arise which will be adressed in the next section. All fibres considered in this section have a width considerably larger than 35 μm.

In Fig. 1 the void volume fraction in extracted gel-spun polyethylene fibres, calculated from the scattering power is presented as a function of different spinning conditions. The contribution of the amorphous/crystalline scattering to the total scattering power was taken into account using an estimated value for the crystallinity of 60% for all fibres. Fibres drawn in the spinline at low spinning temperatures (curve b) have a strikingly high porosity. From previous work [23, 26, 27] it is known that under

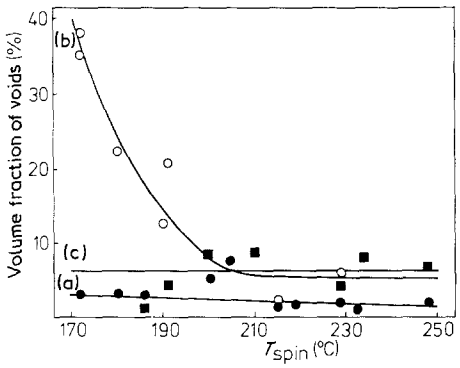

Figure 1 Volume fraction of voids in extracted gel-spun polyethylene fibres as a function of the spinning temperature. The fibres were prepared from a 1.5 wt % Hifax B solution at different spinning conditions. Curve a (●) $V_{spin} = V_{wind} = 100\,m\,min^{-1}$; curve b (○) $V_{spin} = 100\,m\,min^{-1}$, $V_{wind} = 500\,m\,min^{-1}$; curve c (■) $V_{spin} = V_{wind} = 1\,m\,min^{-1}$.

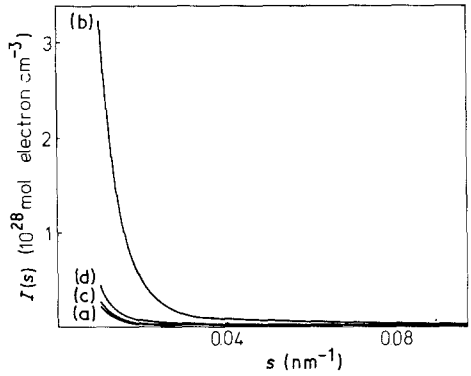

Figure 2 Equatorial SAXS intensity curves of hot-drawn gel-spun polyethylene fibres prepared at different spinning conditions, drawn to different hot-draw ratios, λ, and having different widths, w. Curve a, $T_{spin} = 234°C$, $V_{spin} = V_{wind} = 1\,m\,min^{-1}$, 1.5 wt % Hifax B, $\lambda = 5$, $w = 40\,\mu m$; curve b, the same as a, $\lambda = 50$, $w = 10\,\mu m$; curve c, $T_{spin} = 190°C$, $V_{spin} = V_{wind} = 1\,m\,min^{-1}$, 5.0 wt % Hifax A, $\lambda = 5$, $w = 270\,\mu m$; curve d, the same as c, $\lambda = 50$, $w = 90\,\mu m$. Fibres of curves c and d were spun through a die with a diameter of 2 mm.

these spinning conditions shish-kebab structures are obtained. At higher spinning temperatures this effect decreases and lamellar structures are found. Because the overgrowth of the shish-kebabs prevents a close packing of the backbone fibrils, a very porous structure is obtained. For fibres not stretched in the spinline, a less porous lamellar structure is obtained (Curves a, c). The porosity found can be attributed to the imperfect packing of the large lamellae and the creation of craze-like structures during evaporation of *n*-hexane [23]. The porosity of the fibres spun with a spinning speed of 100 m min^{-1} (curve a) is lower than for fibres spun with a speed of 1 m min^{-1} (curve c). The former ones were prepared at a low polymer concentration and have a ribbon-like shape with the lamellae oriented preferentially with their large flat surface parallel to the ribbon surface [27]. This leads to a more perfect packing of the lamellae. It should be noticed, however, that the calculation of the porosity for these fibres is a rough approximation because the structure is no longer rotational symmetric around the fibre axis.

For some fibres the ratio $\overline{\eta_v^2}/\overline{\eta_p^2}$ was determined and the corresponding volume fraction of voids was calculated using a crystallinity of 60%. Although the differences between the values for the porosity calculated with these two methods can be considerable, the same tendences are observed. For shish-kebab-containing fibres spun at relatively low spinning temperatures, the values for $\overline{\eta_v^2}/\overline{\eta_p^2}$ fluctuate around 35, corresponding to a void volume fraction of about 30%. For lamellar structures this ratio is around 10 corresponding to a void volume fraction of about 5%. One further remark should be added: the maximum dimension of the voids taken into account is approximately 100 nm because a 80 μm entrance slit is used.

3.2. Voids in hot-drawn gel-spun polyethylene fibres

During drawing, the lamellar structures or shish-kebab structures are transformed into more fibrillar-like structures. These fibrillar structures may be more or less closely packed depending on, for example, molecular weight and drawing conditions. For relatively low drawing temperatures, very loosely packed fibrillar structures are obtained, whereas higher drawing temperatures result in more dense structures due to melting/recrystallization [28–32]. The drawing temperature commonly used in our laboratory is in the range 144 to 148° C. During drawing at these temperatures the porosity on a 100 nm scale is largely eliminated [24, 30, 33]. Fig. 2 shows equatorial intensity curves as a function of the scattering vector s for fibres prepared under different spinning conditions, drawn to different hot-draw ratios and having different cross-sectional dimensions. The very high intensity obtained for fibres with a cross-section much smaller than the width of the primary beam is very striking. This is demonstrated again by Fig. 3, where the total scattering power of fibres prepared in different ways is presented as a function of the width of the fibres. The cross-section of a fibre depends on the die diameter, polymer concentration and total draw ratio (i.e. spinline stretching ratio multiplied by the hot-draw ratio).

It is tempting to ascribe the high intensities for thin fibres to a process of void formation during drawing leading to an increasing number of voids with

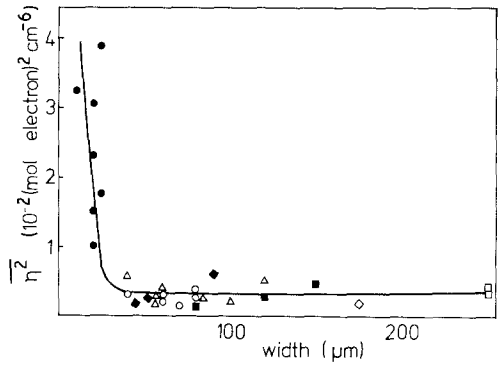

Figure 3 The scattering power of hot-drawn gel-spun polyethylene fibres as a function of the width of the fibres. The fibres were prepared at different spinning conditions and drawn to different hot-draw ratios, λ. (○) $V_{spin} = V_{wind} = 1\,m\,min^{-1}$, $\lambda = 5$, 1.5 wt % Hifax B; (●) $V_{spin} = V_{wind} = 1\,m\,min^{-1}$, $\lambda = 50$, 1.5 wt % Hifax B; (□) $V_{spin} = V_{wind} = 100\,m\,min^{-1}$, $\lambda \approx 5$, 1.5 wt % Hifax B; (■) $V_{spin} = V_{wind} = 100\,m\,min^{-1}$, $\lambda \approx 50$, 1.5 wt % Hifax B; (△) $V_{spin} = 100\,m\,min^{-1}$, $V_{wind} = 500\,m\,min^{-1}$, $\lambda \approx 2$ to 5, 1.5 wt % Hifax B; (◇) $V_{spin} = V_{wind} = 1\,m\,min^{-1}$, $\lambda = 5$, 5.0 wt % Hifax A; (◆) $V_{spin} = V_{wind} = 1\,m\,min^{-1}$, $\lambda \approx 50$, 5.0 wt % Hifax A.

increasing draw ratio [29] but there are a number of observations arguing against this idea. In the first place, fibres spun with a spinning speed of 1 m min^{-1} and drawn to the same hot-draw ratio but having different cross-sectional dimensions due to a different polymer concentration/die diameter show different scattering intensity levels (compare Fig. 2 curves b and d), although their morphology is expected to be approximately the same. It should be noticed that the polyethylene involved in the higher polymer concentration (5 wt %) experiments is a polyethylene with a broad molecular weight distribution (Hifax A: $\bar{M}_w = 4.0 \times 10^6$ kg kmol^{-1}, $\bar{M}_w/\bar{M}_n \approx 20$) whereas for the lower concentration (1.5 wt %) a polyethylene with a narrow molecular weight distribution (Hifax B; $\bar{M}_w = 5.5 \times 10^6$ kg kmol^{-1}, $\bar{M}_w/\bar{M}_n \approx 3$) was used. In the second place, fibres spun with a spinning and winding speed of 100 m min^{-1} originally also having a lamellar structure and hot-drawn to a ratio of about 50, show a low scattering power (Fig. 3). The width of these fibres is relatively large due to their ribbon-like shape [27].

Another possible explanation for the high scattering intensities for very thin fibres is a contribution of reflection of the primary beam on the surface of the fibres to the equatorial scattering curve [34]. This effect may become very important if the surface at which reflection occurs is very close to the centre of the primary beam, i.e. for fibres with small lateral dimensions. Westbrook *et al.* [35] have shown that such effects are present in laminated samples of polystyrene in the grazing incidence region and that this effect may also account for the anomalous scattering observed for crazed polymers [20]. Moreover, they calculated the X-ray refractive index and critical angle for total reflection for polystyrene. The latter turned out to be within the angular region of small-angle X-ray scattering. Because the X-ray refraction index of polyethylene will be very close to the value calculated for polystyrene, the same holds for polyethylene. Such surface scattering may even make a contribution to the scattering of polymers consisting of a stacked lamellae morphology [36]. Whether the high scattering intensity observed for fibres with lateral dimensions smaller than 35 μm can be ascribed to the presence of a considerable number of voids or a contribution of X-ray reflection will be considered next.

From the values of the total scattering power, taking into account the contribution of the scattering due to the electron density difference amorphous/crystalline polyethylene (the crystallinity of the hot-drawn fibres varies between about 30 and 85 wt % [25]), the volume fraction of voids can be calculated which leads to a value of the order of 1% for fibres with a width larger than 35 μm, independent of the spinning conditions. On the other hand, if the high scattering intensity of the thin fibres ($< 35\,\mu$m) is caused by void scattering, this would correspond to void volume fractions up to about 15%.

If voids are present, the corresponding scattering can be eliminated by filling them with paraffin oil. The result of such an experiment for a fibre with a width of 20 μm is presented in Fig. 4. The equatorial intensity of the hot-drawn fibre is suppressed to some extent but

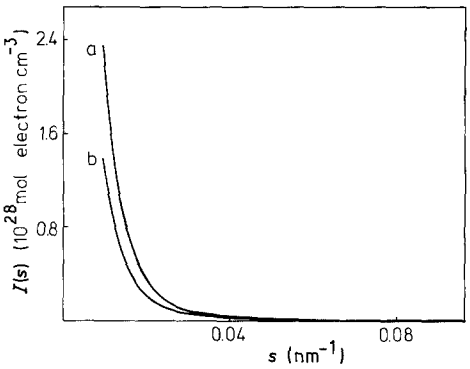

Figure 4 Equatorial SAXS intensity curves of a hot-drawn gel-spun polyethylene fibre prepared from a 1.5 wt % Hifax B solution at a spinning temperature of 248° C and a spinning and winding speed of 1 m min^{-1}. Curve a, $\lambda = 50$; curve b, $\lambda = 50$, fibre filled with paraffin oil.

only for the smaller angles (up to $s \approx 0.06$ nm^{-1}). The intensity reduction is not large enough to account for a volume fraction of voids of about 8% (calculated from the scattering power of the original intensity curve). This is also obvious from the ratio $\overline{\eta_v^2}/\overline{\eta_p^2}$ which is only about 1.5. Moreover, if the scattering results from voids, an intensity reduction over the entire angular range would be expected as was observed for the extracted fibres [23, 24]. A comparable small reduction in intensity is observed for fibres with a width exceeding 35 μm.

The limited reduction may result from an inaccessibility of some of the voids to paraffin oil, for example due to a skin/core effect. However, skin/core effects are expected to become important for relatively thick fibres only. Because the latter show a relatively low scattering power (Fig. 3) this explanation seems not very likely. Another possibility is that the paraffin oil eliminates a small contribution of multiple scattering due to the presence of a not too closely packed macrofibrillar structure with lateral dimensions of the order of micrometres. Such an effect was observed by Perret and Ruland [8, 37] for bundles of carbon filaments with lateral dimensions of the individual filaments of the order of about 5 μm. This results in a multiple scattering contribution to the small-angle X-ray scattering at the smaller angles. Multiple scattering can account for the fact that paraffin oil only suppresses the (multiple) scattering at these angles. Hence, a reflection of the primary beam at the surface of the fibres seems to be the most probable explanation for the high scattering power of thin fibres. In the case of such a macrofibrillar structure, the porosity calculated from small-angle X-ray scattering experiments is no longer representative for the bulk porosity of the fibre but is related to the porosity of the macrofibrils only, which should be calculated from the equatorial intensity curves corrected for the presence of the multiple scattering contribution (i.e. fibres treated with paraffin oil).

The pinhole SAXS pattern of a thin fibre hot-drawn to $\lambda = 40$ is presented in Fig. 5. The intensity is concentrated around the equator in an equatorial streak. This equatorial streak is not characteristic of high hot-draw ratios but is also present at relatively low hot-draw ratios although it is obscured a little by

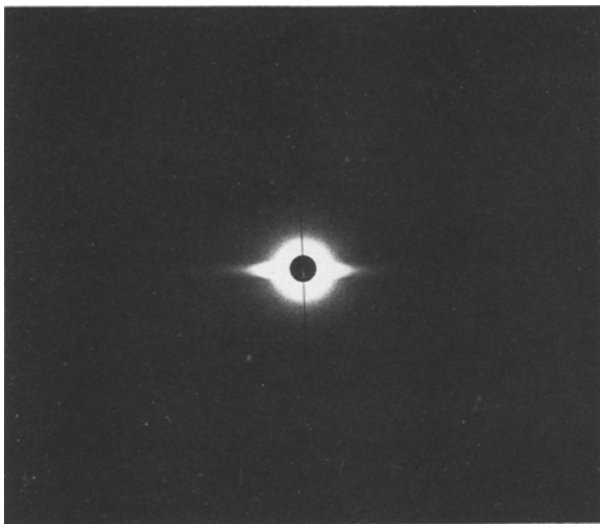

Figure 5 SAXS pinhole pattern of a hot-drawn gel-spun polyethylene fibre prepared from a 1.5 wt % Hifax B solution. The fibre was spun at a spinning temperature of 248° C and a spinning and winding speed of 1 m min^{-1} and afterwards hot-drawn at a temperature of 148° C to a ratio $\lambda = 40$.

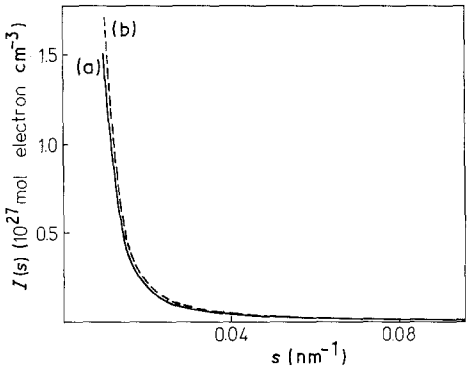

Figure 6 Equatorial SAXS intensity curves of a gel-spun hot-drawn polyethylene fibre (3 GPa) as a function of the strain ratio, ε. The fibre was prepared from a 5.0 wt % Hifax A solution at a spinning temperature of 170° C, a spinning speed of 3.8 m min^{-1} and a winding speed of 2.4 m min^{-1} and hot-drawn to a ratio $\lambda = 75$. The fibre was strained at room temperature, Curve a unstrained; curve b, $\varepsilon = 3.4\%$.

the presence of lamellar material leading to a considerable meridional scattering contribution. Equatorial streaks are often ascribed to void scattering. For example, Kanamoto *et al.* [38] observed a decrease in density of polyethylene films prepared by solid state coextrusion at very high draw ratios. The decrease in density was ascribed to extensive void formation due to fibrillation. The equatorial scattering curve for this film shows an equatorial streak, but these streaks are also clearly visible for much lower draw ratios where the density of the film is much higher. Moreover, the observed scattering pattern differs considerably from the patterns obtained for other elongated void-containing fibres such as cellulose fibres [3] and poly(*p*-phenylene terepthalamide) fibres [12]. This, in combination with low absolute values of the equatorial scattering curves (Figs 2 and 3) leads to the conclusion that a structure containing only a very small volume fraction of voids and a considerable amorphous/crystalline scattering contribution yields equatorial streaks. No indications for the occurrence of superdrawing for draw ratios up to 50 leading to void formation were found. In summary, the results obtained so far clearly indicate that the porosity of hot-drawn fibres drawn in the conventional way is very low (i.e. about 1%).

3.3. SAXS of mechanically stressed gel-spun polyethylene fibres

To study the possible role of void formation in the fracture mechanism of ultra-high-strength polyethylene fibres, a SAXS study of mechanically stressed fibres was carried out. The fibres were strained to different strain ratios and kept at constant length during the scattering experiments. In the case of equatorial experiments, a single fibre was used. For each strain ratio the alignment of the fibre parallel to the slit was checked. In the case of meridional measurements, a bundle of fibres was strained. During the measurements no change of the scattering intensity due to relaxation phenomena could be observed.

Fig. 6 shows the effect of straining a 3.0 GPa polyethylene fibre on the equatorial scattering intensity. Only a very small increase of the equatorial intensity is observed limited to the smaller angles which points to no or very little void formation. This differs considerably from the results of Zhurkov *et al.* [14] who found a high increase of the intensity over the entire angular range for films of oriented polyethylene strained to breakage. Similar results during straining were observed for unoriented polyoxymethylene [15, 16] and hard elastic fibres [17, 18] and were attributed to extensive void formation. Perhaps the difference is due to a difference in the starting morphology. The 3.0 GPa polyethylene fibre used in our experiments has a densely packed highly fibrillar structure whereas the systems showing a high increase of the (equatorial) intensity consists of more (oriented) lamellar structures. The void formation may occur by opening of the space between the lamellae, a mechanism described by Noether and co-workers [17, 18] for hard elastic fibres which consist of well-defined lamellar structures.

To obtain more information about the effect of the morphology of the fibre on the fracture mechanism, a gel-spun hot-drawn polyethylene fibre drawn to a low hot-draw ratio was also studied. This fibre consists of a dense shish-kebab like structure with fibrillar backbones and much lamellar overgrowth as revealed by DSC experiments [25, 39]. In Fig. 7 the meridional scattering curves of these fibres are presented for different strain ratios. This fibre exhibits a clear meridional maximum due to the presence of stackages of lamellae in the lamellar overgrowth oriented parallel to the fibre axis. Upon straining the lamellar period shifts a little to smaller angles and decreases somewhat in intensity but remains visible. No extensive increase of the intensity due to void formation is observed. The same holds for the equatorial scattering curves (not presented here). Most probably the backbone fibrils bear most of the stress during straining which prevents the void formation due to creation of space between

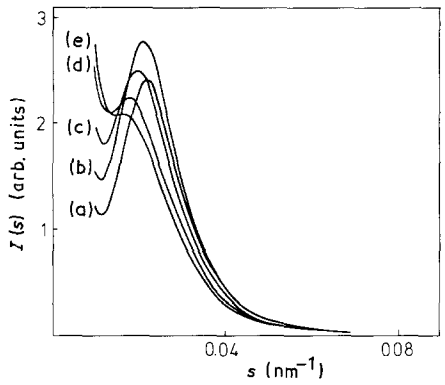

Figure 7 Meridional SAXS intensity curves of a gel-spun hot-drawn polyethylene fibre as a function of the strain ratio, ε. The fibre was prepared from a 5.0 wt % Hifax A solution at a spinning temperature of 170° C, a spinning and winding speed of 1 m min^{-1} and hot-drawn to a ratio $\lambda \approx 5$. The fibre was strained at room temperature. Curve a, unstrained; curve b, $\varepsilon = 5.4\%$; curve c, $\varepsilon = 13.4\%$; curve d, $\varepsilon = 21.8\%$; curve e, $\varepsilon = 26.8\%$.

the packed lamellae. Instead, the deformation is accompanied by shear of neighbouring shish-kebabs leading partly to a distortion of the packages of lamellae oriented parallel to the fibre axis.

4. Conclusion

We have shown that the porosity of extracted gel-spun polyethylene fibres depends on the spinning conditions. The porosity is calculated from the scattering power, obtained from equatorial SAXS experiments, assuming a three-phase system containing voids, amorphous polyethylene and crystalline polyethylene. Shish-kebab structures, obtained after spinline stretching at relatively low spinning temperatures are very porous because a dense packing of the backbone fibrils is prevented by the lamellar overgrowth. On the other hand, extracted lamellae containing fibres consist of more dense structures, especially for fibres spun with a spinning speed of 100 m min^{-1}.

After hot-drawing, the porosity is lost largely (on a 100 nm scale) for both types of fibres as can be concluded from the scattering power which indicates a void volume fraction of about 1%. The small intensity decrease at the smaller angles after a paraffin oil treatment may be due to the elimination of a small contribution of multiple scattering caused by a not too closely packed macrofibrillar structure. If such a structure is indeed present this will result in an underestimation of the porosity of the fibre because the calculation of the porosity from SAXS experiment takes only voids up to about 100 nm into account.

Preliminary SAXS experiments on mechanical strained fibres indicate that no or only very little void formation is involved in the fracture mechanism of ultra-high-strength polyethylene fibres, probably due to the presence of a fibrillar structure.

Acknowledgements

This study was supported by the Netherlands Foundation of Chemical Research with financial aid from the Netherlands Organization for the Advancement of Pure Research.

References

1. P. J. FLORY, *J. Amer. Chem. Soc.* **67** (1945) 2048.
2. A. J. PENNINGS, *Makromol. Chem. Suppl.* **2** (1979) 99.
3. W. O. STATTON, *J. Polym. Sci.* **22** (1956) 385.
4. P. H. HERMANS, D. HEIKENS and A. WEIDINGER, *ibid.* **35** (1959) 145.
5. A. N. J. HEYN, *J. Appl. Phys.* **26** (1955) 519.
6. *Idem, ibid.* **26** (1955) 1113.
7. R. PERRET and W. RULAND, *J. Appl. Crystallogr.* **1** (1968) 308.
8. *Idem, ibid.* **2** (1969) 209.
9. *Idem, ibid.* **3** (1970) 525.
10. C. N. TYSON and J. R. MARJORAM, *ibid.* **4** (1971) 488.
11. A. TAKAKU, M. SHIOYA and J. SHIMUZU, in "Proceedings of the International Symposium on Fibre Science and Technology", Hakone, 1985, p. 190.
12. M. G. DOBB, D. J. JOHNSON, A. MAJEED and B. P. SAVILLE, *Polymer* **20** (1979) 1284.
13. A. M. HINDELEH, N. A. HALIM and K. A. ZIQ, *J. Macromol. Sci. Phys.* **B23** (1984) 289.
14. S. N. ZHURKOV, V. A. ZAKREVSKYI, V. E. KORSUKOV and V. S. KUKSENKO, *J. Polym. Sci. A-2* **10** (1972) 1509.
15. J. H. WENDORFF, *Angew. Makromol. Chem.* **74** (1978) 203.
16. *Idem, Polymer* **21** (1980) 553.
17. H. D. NOETHER and W. WHITNEY, *Kolloid Z. Z. Polym.* **251** (1973) 991.
18. H. D. NOETHER and H. BRODY, *Textile Res. J.* **7** (1976) 467.
19. R. P. KAMBOUR, *Macromol. Rev.* **7** (1973) 1.
20. H. R. BROWN and E. J. KRAMER, *J. Macromol. Sci. Phys.* **B19** (1981) 487.
21. E. PARADES and E. W. FISCHER, *Makromol. Chem.* **180** (1979) 2707.
22. A. J. PENNINGS, R. J. VAN DER HOOFT, A. R. POSTEMA, W. HOOGSTEEN and G. TEN BRINKE, *Polym. Bull.* **16** (1986) 167.
23. W. HOOGSTEEN, G. TEN BRINKE and A. J. PENNINGS, *Polymer* **28** (1987) 923.
24. W. HOOGSTEEN, A. J. PENNINGS and G. TEN BRINKE, *Colloid Polym. Sci.*, in press.
25. W. HOOGSTEEN, G. TEN BRINKE and A. J. PENNINGS, *ibid.* **266** (1988) 1003.
26. W. HOOGSTEEN, R. J. VAN DER HOOFT, A. R. POSTEMA, G. TEN BRINKE and A. J. PENNINGS, *J. Mater. Sci.* **23** (1988) 3459.
27. W. HOOGSTEEN, H. KORMELINK, G. ESHUIS, G. TEN BRINKE and A. J. PENNINGS, *ibid.* **23** (1988) 3467.
28. G. CAPACCIO and I. M. WARD, *Polymer* **18** (1977) 967.
29. L. JARECKI and D. J. MEIER, *J. Polym. Sci. Polym. Phys. Edn* **17** (1979) 1611.
30. J. SMOOK, J. C. TORFS, P. F. VAN HUTTEN and A. J. PENNINGS, *Polym. Bull.* **2** (1980) 293.
31. P. F. VAN HUTTEN, C. E. KONING and A. J. PENNINGS, *J. Mater. Sci.* **20** (1985) 1556.
32. J. SMOOK and A. J. PENNINGS, *J. Appl. Polym. Sci.* **27** (1982) 2209.
33. P. F. VAN HUTTEN, C. E. KONING, J. SMOOK and A. J. PENNING, *Polymer Commun.* **24** (1983) 237.
34. L. G. PARRETT, *Phys. Rev.* **95** (1954) 359.
35. P. A. WESTBROOK, J. F. FELLERS, M. CAKMAK, J. S. LIN and R. W. HENDRICKS, *J. Polym. Sci. Polym. Phys. Edn* **21** (1983) 1913.
36. M. Y. TANG and J. F. FELLERS, *ibid.* **22** (1984) 2215.
37. R. PERRET and W. RULAND, *J. Appl. Crystallogr.* **4** (1971) 444.
38. T. KANAMOTO, A. TSURUTA, K. TANAKA, M. TAKEDA and R. S. PORTER, *Macromol.* **21** (1988) 470.
39. J. SMOOK and A. J. PENNINGS, *Colloid Polym. Sci.* **262** (1984) 712.

Received 16 January
and accepted 24 August 1989